[url]www.elsevier.com

Shear-Force Microscopy Investigation of Roughness and Shape of Micro-Fabricated Holes

Francesco Tantussi[a,*], Daniele Vella[a,1], Maria Allegrini[a], Francesco Fuso[a,2], Luca Romoli[b], Choudhury Abul Anam Rashed[c], Marco Fiaschi[d]

[a] *Dipartimento di Fisica Enrico Fermi, Università di Pisa, Pisa, Italy*
[b] *Department of Industrial Engineering, University of Parma, Parma, Italy*
[c] *Department of Civil and Industrial Engineering, University of Pisa, Pisa, Italy*
[d] *Continental Automotive Italy S.p.A., Pisa, Italy*

Abstract

The paper reports the analysis of roughness and shape of micro-machined workpieces carried out with a specifically conceived scanning probe microscope using the shear-force established between a vibrating tungsten tip and the surface under investigation. Samples, fuel injector nozzles, were prepared by different drilling techniques using either electro-discharge or laser-based machining techniques. Owing to its operation in true non-contact mode and the ability to analyse recessed surfaces, the microscope enables comparing the performance of the drilling processes through the determination of roughness parameters of the hole inner surface and the reconstruction of the shape at its edge. Both finishing and morphological details, expected to be involved in determining the fluid dynamics occurring inside the nozzle, can be captured by the developed diagnostics. The findings reveal that the use of ultrafast laser machining can lead to significantly improve the quality of fuel injector nozzles with respect to the present technology standard.

Keywords: `Scanning Probe Microscopy, Roughness, Laser Machining, Micro-machining`

1. Introduction

In the present technological scenario, there is a continuous demand for the development of new devices able to meet the requirements of evolving standards. Assessment of device and technology performance requires in turn the availability of robust and reliable diagnostic tools. An example is represented by the machining of fuel injector holes in automotive industry. Improving the

*Corresponding author
Email address: `francesco.tantussi@gmail.com` (Francesco Tantussi)
[1] present address: Department for Complex Matter, Jozef Stefan Institute, Ljubljana, SI
[2] present address: Istituto Italiano di Tecnologia, Genova, Italy

efficiency of fuel spray atomisation is mandatory to meet the requirements of the EU6 and forthcoming regulations [1]. Amount and quality of exhaust gas emission from direct injection gasoline engines, as well as reduction of fuel consumption, strongly depend on the geometrical properties of the injector nozzles [2]. Fuel injected through the micro-hole, typically featuring 150-200 μm diameter and 250-350 μm thickness, is assumed to form a liquid core which is then broken-up and atomised into fine droplets. The more complete the atomisation, the cleaner and more efficient the engine operation is, since a properly atomised fuel jet is expected to prevent wet parts in the engine. Atomisation of the fuel spray and jet breaking are governed by the fluid dynamics processes occurring inside the hole, affected by the hole geometry (size, taper angle) as well as by microscopic details of the surface finishing. They include the roughness of the inner surface and the sharpness of the corner edge, which depend on many factors related to both material and process parameters.

Tools capable of investigating the machined surface at the sub-micrometre scale must be used in order to measure the relevant quantities. This need is even more urgent when new machining approaches are being introduced into the industrial environment, as in the case of fuel injector micro-holes. At present, micro-Electrical Discharge Machining (μ-EDM) is a well established technique for drilling nozzles in diesel and gasoline injection systems. The flexibility with respect to workpiece geometry and material is a distinctive advantage of this fabrication approach [3]. Despite of the frequent breakage of electrodes occurring when sharp and very small holes are fabricated [4], it remains the method of choice for drilling hard conductive materials with diameters down to 5 μm. Other machining techniques have been proposed and demonstrated to further improve the process performance and workpiece quality. In particular, techniques based on pulsed lasers have been widely explored. Unique advantages are offered by the use of laser tools such as, the excellent spatial resolution, a good degree of flexibility, and the inherently true non-contact and no tool wear machining due to the use of an immaterial beam [5]. Application of μs and ns laser pulses in the context of industrial micro-fabrication is concerned by the occurrence of large heat affected zones and recast of material [6], preventing the attainment of the required surface quality. The availability of ultra-short laser pulses, with a duration in the sub-ps range, has recently opened the way to circumvent the above mentioned problems, leading to a surface quality even better than in μ-EDM-machined holes. Owing to the very high transient intensity and small heat affected zone induced [7], ultra-short pulses prevent material melting and the consequent recast.

For those reasons, the use of ultrafast laser sources is gaining a strong momentum also for industrial applications. However, due to the relatively recent introduction of laser methods in the field of micro-hole drilling for automotive components, a careful tuning of the process parameters is needed in order to improve the effectiveness of the technique. In addition, its assessment in terms of quality of the machined workpiece requires the ability to reliably compare the surface and shape properties of the laser-machined micro-holes with those obtained through more conventional techniques. Within this context, the abil-

ity to measure roughness and edge sharpness with the required sub-micrometre spatial resolution is a key point to enable the envisioned progresses in process technologies [8]. Unfortunately, access for metrological characterisation is very limited to the inside surface of deep and narrow holes. Highly valuable diagnostics able to measure directly inside the hole have been proposed (see, e.g., [2]). However, despite of its destructive and time wasting nature, sectioning the nozzle along its axis is a commonly used procedure in order to expose a curved and recessed surface to the analysis, as carried out also in the present work.

Scanning Electron Microscopy (SEM) is a precious tool to reconstruct the surface morphology with an extremely large spatial resolution. Shape and size of the holes can be duly analysed by SEM, which, however, is not suited for direct measurement of the surface roughness. Several technical options are available for metrological surface analysis, each approach owning distinctive advantages and disadvantages, whose detailed discussion is out of the scope of the present paper. Conventional stylus profilometers have been around for many years. They have been used to retrieve morphological information also in the context of micro-hole fabrication (see, e.g., [9]), including, for instance, a configuration using a cantilever-type tactile probe sensor able to penetrate into the hole [2]. In stylus profilometers the probe has to be kept in mechanical contact with the investigated surface, that can make probe wear or surface scratching an issue, in particular when corrugated surfaces or soft materials are investigated. Optical profilometry (digital optical microscopy) is a technique developed to avoid the need for contact, while providing a fast two-dimensional morphology reconstruction with an accuracy depending on the actual spatial resolution of the used instrument [12]. According to the experience with the machined parts considered here, the optical approach can be prone to several artifacts, as also reported in the literature (see, e.g., [11]), in particular when surfaces featuring relevant slopes or showing a complicated texture, for instance made of different components, are analysed. In addition, the metrological characterisation of the corner edge and the measurement of its sharpness cannot be achieved with purely optical methods, even though many advancements have been carried out in the field of optical profilometry in the last years, leading to commercial instruments combining different technologies (see, e.g., [10]) for an enhanced versatility.

Scanning Probe Microscopy (SPM), in particular Atomic Force Microscopy (AFM), represents a valuable diagnostics for surface morphology [13] able to obtain accurate roughness information [12]. While being originally conceived for the investigation of atomistically flat surfaces, where atomic resolution has been demonstrated, AFM has also been used in the context of investigation and assessment of machined surfaces (see, e.g., [14, 15, 16]). The performance of AFM has stimulated the development of sophisticated metrological instruments [17], able to determine shape and surface properties with an accuracy exceeding the nanometre level.

According to the experience with the samples considered here, application of conventional AFM to the practical determination of surface finishing in machined workpieces reveals several critical issues. First of all, in the conventional

tapping-mode operation of AFM a fast oscillation is applied to the tip along the vertical direction [18], leading to the possibility of intermittent contact between tip and surface and eventually to tip wearing and material scratching issues. Even though such effects can severely affect the measurements only in the case of soft material analysis, or when ultra-sharp tips are used in order to ensure high spatial resolution (below 10 nm), a true non-contact tool is often desirable. Moreover, large travel capabilities are needed when workpieces with complex shapes are analysed, which are not always found in instruments designed for atomic-scale imaging (typical maximum vertical displacement in AFM is around 5 μm [19]). In addition, the optical lever method generally exploited in AFM can be affected by artifacts due to scattering of stray light from the corrugated surface, particularly relevant in the case of rough metal surfaces. The use of non optical methods for detecting the probe motion can suppress such artifacts while ensuring the ease-of-use required for routine analysis, as often needed in the assessment of machined workpieces. Finally, while flat surfaces can be analysed in a straightforward way by using a conventional AFM, the shape and size of the cantilevered probes can pose physical limitations for accessing recessed surfaces, due to possible mechanical interactions between the cantilever and the edges of the machined workpiece.

The main goal of the present paper is to show the metrological results acquired with a specifically conceived SPM tool, namely a SHear Force Microscope (SHFM), on cross-sectioned micro-holes for fuel injectors. In order to elucidate the capabilities of the instrument, samples machined by different drilling techniques are investigated: μ-EDM, water jet guided laser (WJ), short (ps) and ultra-short (fs) pulse laser machining. The inner surface roughness and the sharpness of the generated edges are compared. The measuring procedure is able to identify standardised values of the surface finishing and to evaluate the crucial parameters defining the shape of the corners of the machined micro-holes.

2. Experimental setup

Approaches based on SHFM allow keeping the advantages in terms of resolution and sensitivity of AFM while virtually eliminating the above mentioned limitations. In SPM technology, shear-forces are conventionally used to sense the surface as in Scanning Near-field Optical Microscopy (SNOM) [20]. Their occurrence and behaviour are mostly due to the viscous interaction of the air layers imprisoned between the tip, kept in oscillation parallel to the surface, and the surface itself. Such an interaction is known to produce a strong damping when the tip-to-surface gap decreases at the few nanometres level [21]. Remarkably, in SHFM the tip is forced to oscillate only in the direction parallel to the sample surface. Therefore, any form of contact is avoided, at least if the oscillation amplitude is kept small enough (below 10 nm in the instrument presented here) compared to the typical spacing of surface features. This prevents tip wearing, improving as a consequence repeatability of measurements, a key point when comparison between different machined surfaces is the main objective of the research. Furthermore, in the absence of vertical oscillations, cantilevered

probes are not needed and can be replaced by needle-like tapered tips suited to approach recessed surfaces and to comply with complex shapes. Finally, sensing the oscillation amplitude can be accomplished by non-optical methods, therefore removing any problem related to stray light scattering and the associated need for time wasting alignment of the optical paths. Commercially available quartz tuning fork can be used to monitor the oscillation amplitude, according to a method originally introduced by Karrai et al. [22] and widely used with tapered optical fibre probes, as those customarily employed in SNOM.

Core of the setup is the probe assembly, which includes the tip, glued to one tuning fork prong, and a piezoelectric transducer needed to put the fork/tip system into a dithering oscillation parallel to the sample surface, as schematically depicted in Fig. 1(a).

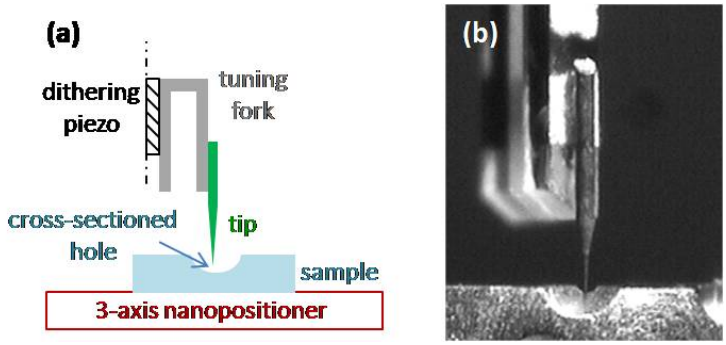

Figure 1: Sketch (a) and picture (b) of the tip and sample arrangement. Note that the drawing in panel (a) is not to scale. For reference, the diameter of the tungsten wire in the non-etched portion, the one glued to the tuning fork prong, is 125 μm.

Tips are made by electrochemical ac-etching a tungsten wire (0.125 mm dia.) in a KOH solution. By properly setting the etching parameters, apical diameters around fifty to one hundred nanometres can be routinely achieved. Smaller apical diameters can be attained by using slightly modified fabrication recipes, which were however not implemented in the present work due to their limited reproducibility. For instance, fabrication of 10 nm tips, as assessed by electron microscopy, was obtained in less than 20% of the produced probes, whereas the method applied here ensured the achievement of apical radii (50$\pm$10) nm in more than 80% of the produced batch. Tips are then epoxy glued on one tuning fork prong. The gluing process, assisted by a set of custom made micro-manipulators, is controlled with an optical microscope. In particular, any unneeded excess of glue on the prong, which can lead to decrease the quality factor of the oscillator, is carefully removed. The length of the probe can be made large enough (up to several tenths of mm) to approach recessed surfaces without accidental interactions of the sample with other parts of the assembly. Increasing the tip length implies a larger mass applied to the tuning fork prong, hence a decrease of the quality factor of the mechanical oscillator. The experimental findings demonstrate reliable operation of the microscope, for the purposes of the investigation

presented here, for tip lengths up to around 10 mm, or slightly above. Figure 1(b) shows a picture of the probe setup in operation on a sectioned hole.

The oscillation is forced at a frequency chosen within the resonance curve of the mechanical system, e.g., detuned by less than 1% from the resonance peak (typically corresponding to around 32 kHz). The signal produced by the tuning fork, duly preamplified, is synchronously AM-demodulated by a lock-in amplifier (EG&G 9503) in order to obtain a dc-signal proportional to the mechanical oscillation amplitude. The dc-signal is sent to a feedback electronics, included in a commercial SPM controller (RHK-spm100). There, it is continuously compared to a set-point value, normally chosen around 80% of the free oscillation value. The output of the feedback circuit, duly conditioned, governs the vertical displacement of the sample. Therefore, constant tip-to-sample gap operation is achieved, preventing any accidental tip to surface contact.

The sample is placed on a 3-axis piezoelectric nanopositioner (Physik Instrumente mod. 517), which, owing to the implementation of capacitive sensors, operates in closed loop. The same nanopositioner enables both vertical, feedback-controlled, displacement, and raster scanning of the sample under the tip. The maximum travel is 100 μm$\times$ 100 μm in the in-plane (scan) directions, whereas the maximum vertical displacement is 20 μm. Joined with the large physical accessibility to the sample under investigation, this enables analysing workpieces with complex geometries and relatively large size, including the metrological characterisation of the corner edge.

During a raster scan of the sample, the SHFM reconstructs the topography map as an $h_{i,j}$ matrix. The $h_{i,j}$ (height) value is achieved at any i, j measurement point upon the requirement of the constant gap established by the feedback system, and is calibrated according to the positional accuracy of the nanopositioner (0.1 nm, nominal, along the vertical direction). Usually, the fast scan, along the x direction (rows), is set orthogonal to the hole axis. The slow scan, along the y direction (columns), is therefore parallel to the hole main axis. The instrument is equipped with two long working-distance, high magnification CCD cameras mounted along two mutually orthogonal directions for coarse positioning the sample with respect to the tip.

The in-plane spatial resolution of the microscope depends on the sharpness of the tip, which can be determined by scanning a calibration standard (MikroMasch TGT-01) comprising an array of silicon-based spikes with known geometry. Due to the sharpness of such spikes (featuring a nominal radius of curvature below 10 nm), the scan provides with an inverted image of the apical part of the tip [23]. As-prepared probes used in the present investigation show an apical (tip) radius below 60 nm. Such a value, larger than the typical apical radius of conventional scanning probe microscopes, is adequate for the purposes of the presented research, as demonstrated by the results which will be discussed in the following section.

Reliability of the measurements has been checked by carrying out several tens of subsequent scans on the same portion of one of the samples under investigation. Relative variations of the roughness parameters have been found to be below $\pm$5% (roughly corresponding to $\pm$ 5 nm in the evaluation of the

root-mean-square roughness, S_q) on the basis of over 30 repeated scans of the same portion of the sample. The reported value represents an estimation of the uncertainty for the obtained measurements of the roughness parameters. The noise floor of the instrument was ascertained through repeated scans of smooth test samples (silicon wafers) accomplished in the same experimental conditions of the analysis presented here. Height fluctuations within ± 2 nm were found, ascribable to electronic noise and to the presence of mechanical vibrations and thermal drifts in the setup.

3. Morphology of the inner surface of the micro-hole

Prior to morphological imaging, a flattening procedure is applied to remove the global curvature due to the circular shape of the hole. To this aim, a two-dimensional best-fit is applied and the resulting flattening surface subtracted to the raw data. Typically, a second-order polynomial function is used; using a higher degree polynomial does not lead to any remarkable difference. The procedure makes the surface to be projected over a flat plane. An example is shown in Fig. 2, where a pseudo-3D representation produced by a specific software [24] is presented (maps refer to a hole μ-EDM-drilled into stainless steel).

Remarkably, the flattening procedure removes any possible effect associated with the non perfect alignment of the tip along the direction normal to the scan plane on the determination of the roughness parameters. This has been assessed by selecting a region on a sample and performing scans for different angles of the tip, purposely misaligned with respect to the normal to the scan plane by approximately ± 15 degrees (the maximum inclination of the investigated regions is below 30 degrees). The consistency of the roughness parameter evaluation was checked: in all cases, the obtained parameters showed a variation within the above reported uncertainty (± 5%). Misalignment of the surface for larger angles leads to variations above the mentioned value. For this reason, scans of very inclined portions of the samples, as for instance realised in the analysis of the hole edge, were not used for retrieving roughness parameters.

The flattened maps are useful for a visual comparison of the finishing properties produced by the machining process, as shown in Fig. 3(a-d). In this example, holes produced with the four drilling techniques considered in this paper are compared, demonstrating the capabilities of the SHFM to identify and measure the morphological features of each sample down to the nanoscale. Close to every map, the colour scale for the height reference is represented, dark colours corresponding to lower surface areas (e.g., valleys, craters) and white areas to higher peaks. No low-pass filtering has been applied to the data in order to avoid any loose of spatial resolution.

Cross-sections of the maps along selected segments, representative of the overall behaviour, are shown for instance in Fig. 3(e). The qualitative outcome of the comparison is immediate because the SHFM operating conditions are the same for all scans. Machining with ps and μ-EDM techniques generates considerably more perturbed surfaces. For instance, the μ-EDM-drilled hole

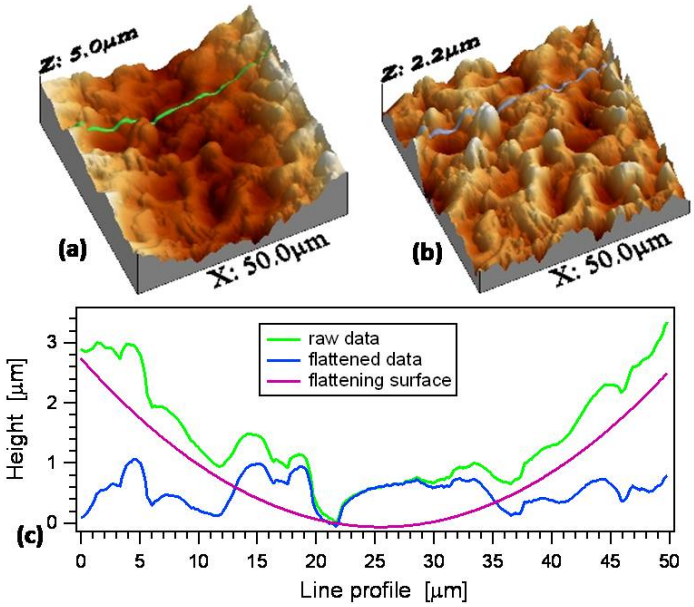

Figure 2: Pseudo-3D representation before (a) and after (b) the flattening procedure described in the text. The graph in panel (c) shows the cross sections of the topography maps, drawn along the segments superposed onto the maps, and of the flattening surface found by the best-fit procedure. Scan parameters for both maps: line speed 5.0 μm/s, 256 $\times$ 256 pixels, total duration 43 min.

shows a topography whose maximum excursion is on the order of 1 μm, roughly five times larger than for holes drilled by WJ and fs techniques.

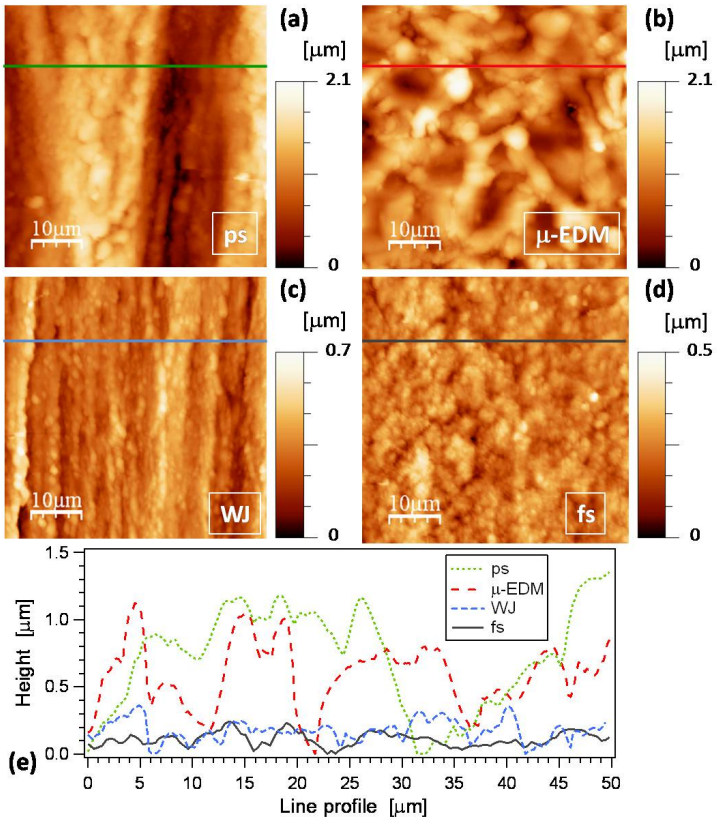

Figure 3: SHFM topography maps acquired on holes drilled by different techniques: ps-laser (a), μ-EDM (b), water-jet guided laser (c), and fs-laser (d). Cross sections along the segments superposed to the maps (e). Scan parameters for all maps: line speed 8.0 μm/s, 256 $\times$ 256 pixels, total duration 27 min.

3.1. Areal roughness parameters

For a more detailed analysis, suitable for comparative purposes, the finishing properties of the investigated surfaces can be summarised by using conventional roughness parameters [25, 26]. The analysis is carried out averaging over the whole map, leading for instance to the root-mean-square height, S_q [3, 27] representative of the surface-averaged roughness induced by the machining process. Results reported in Table I, based on the whole set of scans carried out on different samples, clearly indicates that fs-machining ensures the lowest surface-averaged roughness, roughly a factor 5 smaller than for the standard μ-EDM process. Conversely, the use of longer laser pulses (ps) produces an even more

pronounced roughness. Finally, WJ-machining leads to better results in comparison with standard μ-EDM, but the roughness is still larger than for fs-laser pulse machining. As visually suggested by the images shown in Fig. 3, the overall dynamics of the topography, represented by the S_t parameter (also known as S_z [26]) reported in Table I, follows a similar trend, even though variations from one to another machining technique are in this case less evident than for S_q.

There is another important information directly provided by the topography maps. It is clear that ps and WJ processes produce a strong anisotropy in the surface texture. Elongated morphological features roughly aligned along the vertical direction of the scan, corresponding to the hole main axis, are observed in the maps of Fig. 3(a) and (c). The occurrence of such anisotropy is confirmed and quantitatively measured through a statistical analysis based on Auto-Correlation Function (ACF) maps. The normalised ACF matrix is defined as

$$A_{i',j'} = \frac{\Sigma_{i,j} h_{i,j} h_{i+i',j+j'}}{\Sigma_{i,j} h_{i,j}^2} \ . \tag{1}$$

The map of the $A_{i',j'}$ matrix gives a measure of the in-plane correlation length between the features detected in the topography maps. For instance, in the case of a periodical array of features, a regular array is reproduced in the ACF map, with a spacing corresponding to the period of the original features. In the more interesting case of non periodical arrays, the ACF matrix is still able to provide information relevant to characterise the topography. The corresponding maps present a central peak, as shown for instance in Fig. 4, displaying the ACF matrices obtained from the topographies reported in Fig. 3(a-d). The peak, with a normalised (unity) amplitude, displays a shape which is an indicator of the texture anisotropy. A threshold, typically set at 0.2, is applied to the map and two quantities R_{min} and R_{max} are identified as, respectively, the minimum and the maximum distance from the origin of the portion of the central peak remaining visible after the thresholding process [28]. The fastest decay autocorrelation length [26], $S_{al} = R_{min}$, and the texture aspect ratio [26], $S_{tr} = R_{min}/R_{max}$, obtained from the analysis are reported in Table I.

The fastest decay autocorrelation length, S_{al}, gets comparatively small values for the μ-EDM and, in particular, for the ultrafast laser drilling (fs). The latter is a clear signature that a dense surface texture made of relatively small features occurs following the interaction with the laser pulses. Recast of molten material, expected to produce larger features, is effectively prevented due to the short duration of the interaction and the subsequent small extent of the heat affected zone. The texture aspect ratio parameter, S_{tr}, could not be evaluated for samples drilled by ps and WJ techniques, at least by setting the threshold at 0.2. Only an upper bound for the parameter could be estimated ($S_{tr} < 0.1$ for both techniques), since the elongated features extend practically for the whole length of the drilled hole.

Owing to the geometrical arrangement of the scans, where the vertical axis coincides approximately with the hole main axis, it is possible to reconstruct

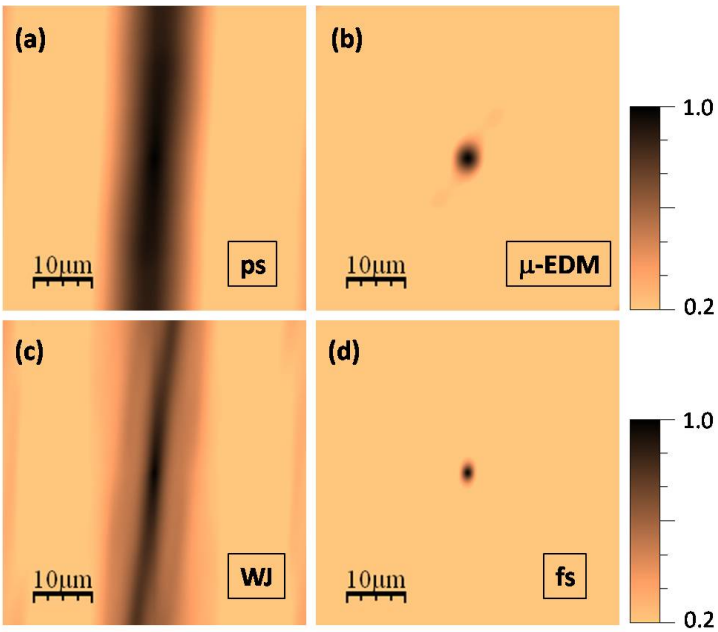

Figure 4: Maps of the normalised autocorrelation function (ACF) for the topographies shown in Fig. 3(a-d). Samples are produced using ps-laser (a), μ-EDM (b), water-jet guided laser (c), and fs-laser (d). The color scale of the maps is adjusted in order to span from 0.2 to 1, i.e., from the threshold to the peak amplitude.

Parameter	Technique				Unit
	ps	EDM	WJ	fs	
S_q	410	340	89	73	[nm]
S_t	2.0	2.2	0.7	0.6	[μm]
S_{al}	11	2.9	8.6	1.4	[μm]
S_{tr}	NA	0.61	NA	0.66	

Table 1: Table I. Roughness parameters determined for samples machined by different drilling techniques.

the evolution of the roughness along the drilling direction. To this aim, several scans have been carried out on the samples in order to image the inner surface of the micro-hole along its whole length (150 μm). Then, the root-mean-square roughness, R_q [25], has been evaluated for every row, that corresponds to R_q at a certain distance from the beginning of the hole.

An example of the results is shown in Fig. 5, where the evolution of the roughness with the drilling penetration is shown for samples produced by the four drilling techniques considered here. Besides the already presented differences in terms of produced roughness, it is clear from the plot how the fs-laser technique leads to finishing properties which remains almost constant while the drilling proceeds to its end. On the contrary, in ps and WJ techniques the roughness tends to increase with the hole depth. Finally, μ-EDM drilled holes show marked fluctuations in the roughness value, preventing the identification of any trend.

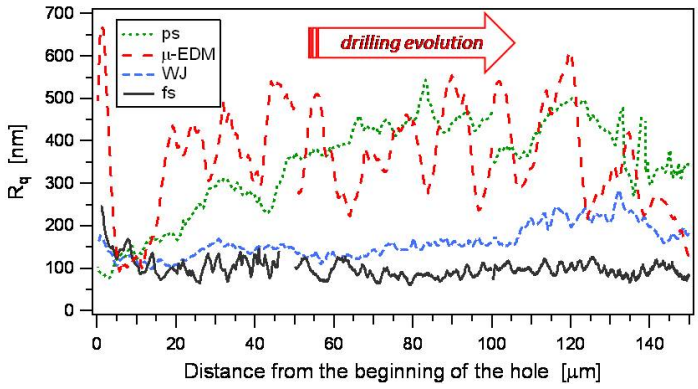

Figure 5: Plots of the root-mean-square roughness R_q evaluated along 50 μm-long segments roughly directed orthogonally to the hole main axis as a function of the distance from the beginning of the hole. The drilling direction proceeds from left to right. Lines correspond to samples machined by different drilling techniques, as specified in the legend. Plots are obtained from the analysis of three distinct scans. Raw data, with no gluing, are used that explains the line discontinuities.

This can be interpreted as a consequence of the physical mechanisms involved in the processes. Using the ultrafast laser, drilling conditions are kept almost constant during the hole finishing process; negligible material recast occurs which could eventually lead to modify the surface encountered by the drilling beam. As already mentioned, a relatively long duration of the laser pulses, like in the ps-laser technique, while promoting an efficient material removal, is accompanied by remarkable modifications of the surface, where pulse after pulse material is eventually re-deposited. A similar behaviour can be hypothesised also for the water-jet guided laser machining, where, in addition, material removal induced by the water jet is affected by the hole depth as well. Its efficiency is expectedly reduced when the jet must travel along the entire hole length. Finally, the roughness produced by the μ-EDM technique can be

associated with local fluctuations of the removal efficiency, not related with the depth of penetration of the electrode inside the hole. However, the extent of such fluctuations could mask any penetration-depending behaviour.

3.2. Edge sharpness analysis

The non-obtrusive method based on shear-forces, joined with the absence of (unwanted) physical interference between the sensor and the sample, enable using SHFM also for carrying out metrological analysis of the machined samples aimed at determining their shape with sub-micrometre spatial resolution. Within the context of fuel injector fabrication, sharpness of the edge at the end of the hole, typically set by design to produce a 90 degrees corner, is a very relevant factor. In particular, the radius of curvature at the edge is expected to strongly affect the fluid dynamics of the injection process, being related to cavitation, generation of vortices, and, more in general, to the spray atomisation process. The radius of curvature depends on many parameters involving both the material properties and the local features of the interaction with the ablating beam.

Owing to the sufficiently large travel range enabled by the nanopositioner, SHFM scans can be carried out on the area across the edge of the nozzle providing a direct measurement of the angle and of its radius of curvature. By subsequently scanning several rectangular areas across the edge, the uniformity of the radius along the hole circumference can also be evaluated. Such a kind of measurements does not require any modification to the instrumental setup, which is able to accommodate for sample holders offering access to the area of interest. Fig. 6(a) reports a picture of the tip and sample arrangement in the configuration used for the analysis.

As an example, Fig. 6(b,c) shows two maps acquired on the edge of holes. In this case, the analysis has been carried out only on samples machined by fs (b) and μ-EDM (c) techniques, representing the future alternative and the present standard drilling tool, respectively. The edge of the corner is clearly visible as a relatively sharp protrusion roughly located at the centre of the maps and aligned along the vertical direction. The left side of the map with respect to the edge corresponds to the nozzle, the right side to the outer part of the device.

The cross-sections of the maps, extracted along the segments superposed to the images, are shown in Fig. 6(d,e). In order to characterise the angle, a best-fit of the left and right portions of each cross section to straight lines is carried out, shown in the plots as dotted lines. The angle included between the prolongations of such lines, representing the overall angle of the corner over the whole length of the cross section (30 μm, for the shown examples), is found in the range 65-75 degrees, independently of the drilling technique. The evaluation of the radius of curvature at the edge is then performed by making a best-fit to a circle function of the portion of the cross section markedly diverging from the straight lines. The choice of the fitting function has not been done in order to obtain the best possible agreement with the topography data, but rather to find a parameter able to characterise the morphology of the edge. Large curvature

radius indicate a smooth corner, whereas small curvature radius are associated to sharp edges. The results of the best fit are shown as dotted lines in the plots.

The ability of the fs technique to produce rather sharp edges is evident. Radii on the order of 0.6 μm, or even smaller, can be achieved. On the contrary, the μ-EDM technique cannot reach similar promising results and suffers also of a strong inhomogeneity of the edge shape. In the set of investigated samples, radii ranging through 1.2 μm to 4 μm are obtained. Furthermore, as shown in Fig. 6(c), the ability of the instrument to detect topography variations also in strongly inclined surfaces indicates that μ-EDM-drilled micro-holes suffer from relevant morphological inhomogeneities close to the edge. They can be ascribed to the already mentioned local fluctuations of the material removal efficiency, which, according to the presented results, are particularly relevant at the bottom of the drilled hole. Conversely, ultrafast laser machining reveals a much larger accuracy in defining the edge of the hole, due to the negligible effect of material recast and to the ability to precisely direct the ablation of the material.

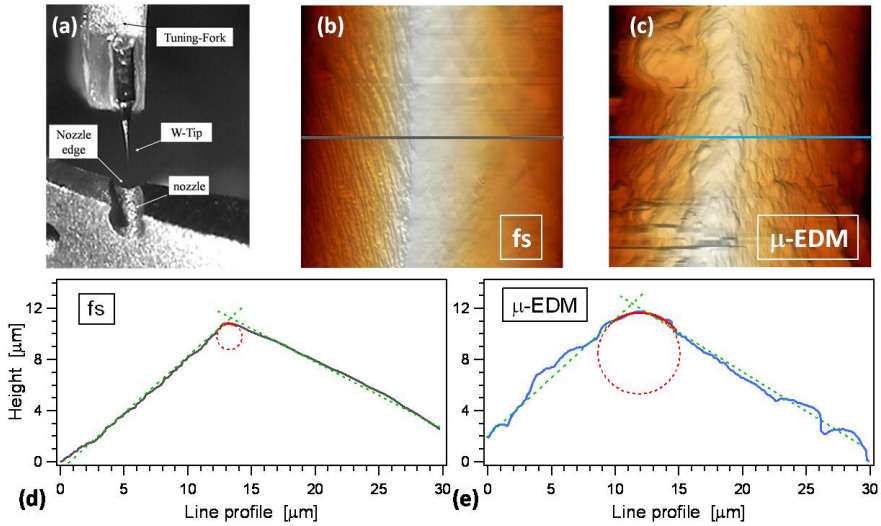

Figure 6: Picture of the tip and sample arrangement for the analysis of the nozzle edge (a). SHFM topography maps acquired on samples machined by fs (b) and μ-EDM (c) techniques. Scan size for both maps is 30 μm $\times$ 30 μm and the vertical excursion is over 12 μm. Cross-sections of the maps along the superposed segments for fs (d) and μ-EDM (e) drilled samples. Dashed and dotted lines represent the results of the best-fit procedure discussed in the text. Scan parameters for both shown maps: line speed 2.0 μm/s, 256 $\times$ 64 pixels, total duration 16 min.

4. Conclusions

In the original implementation presented here, the SHFM is a powerful tool for roughness investigation of complex shape surfaces and for metrological characterisation of the hole edge. Topography maps are obtained by true non-contact

operation and in the absence of the technical limitations and artifacts which could be found when using conventional AFMs for analysing machined surfaces. The topography maps and the subsequent roughness analysis enable assessing the performance of different drilling techniques through a comparison of the obtained features imaged at the sub-micrometre scale in the same measurement conditions.

Results can be of great interest to highlight crucial issues of machining techniques and, more in general, to help obtaining a high control of the manufacturing process. Therefore, the SHFM can acquire a relevant role as a complementary technique to other diagnostics, such as, SEM, optical microscopy, with the added value of providing the user with reliable quantitative data. On the other hand, a detailed knowledge of the morphology of the inner surface of a hole and of its edge can feed fluid dynamics models with realistic surface features, opening the way to an accurate prediction of the actual functional behaviour of the injector nozzle. Efforts are presently devoted to extend SHFM usability to the realm of nano-tribological analysis, where the occurrence of controlled oscillations of the tip along the direction parallel to the surface can be useful for sensing friction effects at the local scale.

5. Acknowledgments

We gratefully acknowledge the financial and technical support of the Continental Automotive Italy S.p.A. Assistance to the measurements by F.Pallesi is also gratefully acknowledged.

References

[1] A. Kufferath, S. Berns, J. Hammer, R. Busch, M. Frank, A. Storch, The EU6 Challenge at GDI - Assessment of feasible systems solutions, Proceedings of the 33rd Internationales Wiener Motorensymposium (2012).

[2] E. Peiner, M. Balke, L. Doering, Form measurement inside fuel injector nozzle spray hole, Microelectronic Engineering; 86, 984-986, (2009).

[3] C.A.A. Rashed, L. Romoli, F. Tantussi, F. Fuso, L. Bertoncini, M. Fiaschi, M. Allegrini, G. Dini, Experimental optimization of micro-electrical discharge drilling process from the perspective of inner surface enhancement measured by shear-force microscopy, CIRP Journal of Manufacturing Science and Technology; 7, 11-19, (2014).

[4] D.T. Pham, S.S. Dimov, S. Bigot, A. Ivanov, K. Popov, Micro-EDM Recent Developments and Research Issues, Journal of Materials Processing Technology; 149, 50-57, (2004).

[5] S. Tao, B. Wu, S. Lei, A comparative study of the interaction between microhole sidewalls and the plasma generated by nanosecond and femtosecond laser ablation of deep microholes, Journal of Manufacturing Processes; 14, 233-242, (2012).

[6] F. Dausinger, Precise drilling with short pulsed lasers, High-Power Lasers in Manufacturing, Proceedings of SPIE; 3888, 180-187,(2000).

[7] Y. L. Yao, H.L. Chen, W. Zhang, Time scale effects in laser material removal: A review, International Journal of Advanced Manufacturing Technology; 26, 598-608, (2005).

[8] C. Diver, J. Atkinson, H.J. Helml, L. Li, Micro-EDM drilling of tapered holes for industrial applications, Journal of Materials Processing Technology; 149, 296-303, (2004).

[9] M.C. Malburg, D.G. Chetwynd, J Raja, Local slope analysis in the stylus-based assesment of surface integrity, Tribology International; 30, 527-532, (1997).

[10] See, for instance, `http://www.bruker.com, http://www.sensofar.com, http://www.alicona.com`.

[11] M. Conroy and J. Armstrong, A comparison of surface metrology techniques, Journal of Physics: Conference Series; 13, 458-465 (2005).

[12] C.Y. Poon and B. Bhushan, Comparison of surface roughness measurements by stylus profiler, AFM and non-contact optical profiler, Wear; 190, 76-88 (1995).

[13] B. Bhushan (Ed.), Springer Handbook of Nanotechnology, Third ed., Springer-Verlag, Heidelberg, New York, 2010.

[14] Y.H. Guu, AFM Surface imaging of AISI D2 tool steel machined by the EDM process, Applied Surface Science; 242, 245-250, (2005).

[15] Y. Xing, J. Deng, Y. Lian, K. Zhang, G. Zhang, and J. Zhao, Multiple nanoscale parallel grooves formed on Si3N4/TiC ceramic by femtosecond pulsed laser, Applied Surface Science; 289, 62-71, (2014).

[16] T. Ghrib, S.B. Salem, Y. Noureddine, EDM effects on the thermal properties of 36NiCrMo16 steel, Tribology International; 42, 391-396, (2009).

[17] A.D. Mazzeo, A.J. Stein, D.L. Trumper, R.J. Hocken, Atomic force microscope for accurate dimensional metrology, Precision Engineering; 33, 135-149 (2009).

[18] Q. Zhong, D. Innis, K. Kjoller, V.B. Elings, Fractured polymer/silica fiber surface studied by tapping mode atomic force microscopy; Surface Science Letters 290, L688-L692 (1993).

[19] See, for instance, R.R.L. De Oliveira, D.A.C. Albuquerque, T.G.S. Cruz, F.M. Yamaji, F.L. Leite. Measurement of the Nanoscale Roughness by Atomic Force Microscopy: Basic Principles and Applications, Atomic Force Microscopy - Imaging, Measuring and Manipulating Surfaces at the Atomic Scale, Dr. Victor Bellitto (Ed.), ISBN: 978-953-51-0414-8, InTech (2012), DOI: 10.5772/37583.

[20] See, for instance, L. Novotny and B. Hecht, Principles of Nano-optics, Cambridge University Press, New York, 2006.

[21] K. Karrai and I. Tiemann, Interfacial shear force microscopy, Physical Review B; 62, 13174-13181, (2000).

[22] K. Karrai, Grober, R.D.. Piezoelectric tip-sample distance control for near field optical microscopes, Applied Physics Letters; 66, 1842-1844, (1995).

[23] V. Bykov, A. Gologanov, V. Shevyakov, Test structure for SPM tip shape determination, Applied Physics A; 66, 499-502 (1998).

[24] I. Horcas, R. Fernandez, J.M. Gomez-Rodriguez, J. Colchero, J. Gomez-Herrero. A.M. Baro, Review Scientific Instruments; 78, 013705-1-8 (2007).

[25] E. Degarmo, B.J.T. Paul, R.A. Kohser, Materials and Processes in Manufacturing (9th ed.), Wiley; 223, ISBN 0-471-65653-4 (2003).

[26] ISO 25178: Geometric Product Specifications (GPS) Surface texture: areal.

[27] C.A.A. Rashed, L. Romoli, F. Tantussi, F. Fuso, M. Burgener, G. Cusanelli, M. Allegrini, G. Dini, Water jet guided laser as an alternative to EDM for micro-drilling of fuel injector nozzles: A comparison of machined surfaces, Journal of Manufacturing Processes;15, 524-532(2013).

[28] R. Leach, Characterisation of areal surface texture, Springer, Berlin, Heidelberg, New York, 2013.